

Correlation of Lesions Evaluated as Sternal Metastases on the Computed Tomography of the Thorax with Primary Malignancies of Patients

Bilgisayarlı Toraks Tomografisinde Sternal Metastaz Olarak Değerlendirilen Lezyonların Hastaların Primer Maligniteleri ile Korelasyonu

¹Nevin Aydın, ²Ilknur Ak Sivrikoz, ¹Suzan Saylısoy, ³Meryem Cansu Sahin, ¹Busra Yavuz, ¹Cuneyt Calisir, ⁴Burcu Atalay, ⁴Didem Arslantas, ⁵Emine Dundar

¹Eskisehir Osmangazi University, Faculty of Medicine, Department of Radiology, Eskisehir, Turkey
²Eskisehir Osmangazi University, Faculty of Medicine, Department of Nuclear Medicine, Eskisehir, Turkey
³Kutahya Health Sciences University Training and Research Center, Kutahya, Turkey
⁴Eskisehir Osmangazi University, Faculty of Medicine, Department of Public Health, Eskisehir, Turkey
⁵Eskisehir Osmangazi University, Faculty of Medicine, Department of Pathology, Eskisehir, Turkey

Abstract: Background: The sternum is a bone in which many malignancies metastasize. Our aim was to evaluate sternal metastases according to the CT characteristics and correlate them with the primary malignancies of patients. The location of metastases was grouped according to sternal anatomy. The metastases in the sternum and other non-sternum bones were classified as lytic, sclerotic, and mixed. Sternal metastases were grouped according to their primary malignancy. For sternal metastases, the maximum standard uptake value (SUVmax) was measured on PET-CT. The presence of metastases in the lung parenchyma was evaluated when sternum metastases were detected. The data obtained from the study were transferred to a computer and evaluated using a statistical package program (SPSS version 15.0) at a statistical significance value of $p \leq 0.05$. Among the 69 patients, the primary diagnosis was lung cancer in 29.0% (n=20), prostate cancer in 27.5% (n=19), and breast cancer in 21.7% (n=15). In the sternum localization, the CT imaging revealed corpus involvement in 89.8% (n=62), manubrium involvement in 57.9% (n=40), and xiphoid involvement in 11.6% (n=8). The maximum lesion density ranged from 26 to 974 HU with a median of 352 HU. The maximum lesion diameter ranged from 3.0 to 32.1 mm in the axial section, with a median of 11.61 mm. The most common type of metastasis was sclerotic (60.9%) in the sternum and was multiple sclerotic (50.7%) in non-sternum bones. Of the patients, 15.9% (n=11) had metastasis both in the sternum and lung parenchyma. The most common corpus sternum involvement was found in lung cancer, while manubrium and xiphoid involvement was most observed in prostate cancer. Sclerotic metastasis involvement was also most frequent in prostate cancer. Lesion density was higher in prostate cancer than other types of cancer. No difference was found between the types of cancer in terms of the diameter of lesions in the axial section or the measured SUVmax values. CT is an important diagnostic tool in the detection of sternum metastases and should be correlated with PET-CT. It should be kept in mind that low SUVmax values can be obtained, especially in lung cancers. Among primary malignancies, corpus sternum metastasis was most common in lung cancers and manubrium and xiphoid metastases in prostate cancers. Furthermore, corpus sternum involvement was found to be the most common localization, indicating that especially the corpus sternum should be carefully evaluated in the scanning of metastases.

Keywords: breast cancer, MCF-7, PLA, PET, 3 dimensional, scaffold, cell culture

Aydın N, Ak Sivrikoz I, Saylısoy S, Sahin MC, Yavuz B, Calisir C, Atalay B, Arslantas D, Dundar E, 2020. Correlation of Lesions Evaluated as Sternal Metastases on the Computed Tomography of the Thorax with Primary Malignancies of Patients, *Journal of Medical Innovation and Technology*

Özet: Sternal metastazları BT özelliklerine göre değerlendirmek ve hastaların primer maligniteleriyle ilişkilendirmek. Çalışma Tasarımı: Metastazların yeri sternal anatomiye göre gruplandırıldı. Sternum ve diğer sternum olmayan kemiklerdeki metastazlar litik, sklerotik ve karışık olarak sınıflandırıldı. Sternal metastazlar primer malignitelere göre gruplandırıldı. Yöntemler: Sternal metastazlarda maksimum standart alım değeri (SUVmax) PET-CT'de ölçüldü. Sternum metastazları tespit edildiğinde akciğer parankiminde metastaz varlığı değerlendirildi. Çalışmadan elde edilen veriler bir bilgisayara aktarılmış ve istatistiksel paket değeri (SPSS sürüm 15.0) kullanılarak $p \leq 0.05$ istatistiksel anlamlılık değerinde değerlendirilmiştir. Bulgular: 69 hasta arasında birincil tanı% 29.0 (n = 20) akciğer kanseri,% 27.5 (n = 19) prostat kanseri ve% 21.7 (n = 15) meme kanseri idi. Sternum lokalizasyonunda BT görüntülemesinde% 89.8 (n = 62) 'te korpus tutulumu,% 57.9' da manubrium tutulumu (n = 40) ve% 11.6 (n = 8) 'de ksifoid tutulumu saptandı. Maksimum lezyon yoğunluğu 26 ila 974 HU arasında değişmekteydi ve ortalama 352 HU idi. Maksimum lezyon çapı, eksenel kesitte 3,0 ila 32,1 mm arasındaydı ve ortalama 11,61 mm idi. En sık görülen metastaz tipi sternumda sklerotik (% 60.9) ve sternum dışı kemiklerde multipl sklerotik (% 50.7) idi. Hastaların% 15.9'unda (n = 11) hem sternumda hem de akciğer parankiminde metastaz mevcuttu. En sık görülen korpus sternum tutulumu akciğer kanserinde, manubrium ve ksifoid tutulumu en çok prostat kanserinde görülmüştür. Sklerotik metastaz tutulumu prostat kanserinde de en sık görülmüştür. Lezyon yoğunluğu prostat kanserinde diğer kanser türlerine göre daha yüksekti. Aksiyal kesitteki lezyonların çapı veya ölçülen SUVmax değerleri açısından kanser türleri arasında fark bulunmadı. Sonuçlar: BT sternum metastazlarının saptanmasında önemli bir tanı aracıdır ve PET-BT ile korelasyon göstermelidir. Özellikle akciğer kanserlerinde düşük SUVmax değerlerinin elde edilebileceği unutulmamalıdır. Primer maligniteler arasında akciğer kanseri ve prostat kanserlerinde manubrium ve ksifoid metastazlarda en sık korpus sternum metastazı saptandı. Ayrıca, korpus sternum tutulumunun en yaygın lokalizasyon olduğu saptanmıştır, bu da özellikle korpus sternumun metastazların taranmasında dikkatle değerlendirilmesi gerektiğini göstermektedir.

Anahtar Kelimeler: Sternum, Metastaz, bilgisayarlı tomografi, Pozitron Emisyon Tomografisi, Toraks

Aydın N, Ak Sivriköz İ, Şaylısoy S, Şahin MC, Yavuz B, Çalışır C, Atalay B, Arslantaş D, Dündar E, 2020. Bilgisayarlı Toraks Tomografisinde Sternal Metastaz Olarak Değerlendirilen Lezyonların Hastaların Primer Maligniteleri ile Korelasyonu, *Medikal İnovasyon ve Teknoloji Dergisi*

ORCID ID of the authors: N.A 0000-0002-7765-4323, İ.A.S 0000-0002-5133-9931, S.Ş 0000-0002-1560-964X, M.C.Ş 0000-0002-5743-3734, B.Y 0000-0002-0818-7426, C.C 0000-0002-2763-4906, B.A 0000-0001-9149-6424, D.A 0000-0002-5263-3710, E.D 0000-0001-5675-0124

Received 05.06.2020

Accepted 11.06.2020

Online published 15.06.2020

1. Introduction

The sternum consists of three parts comprising the manubrium, corpus, and xiphoid process, and it is a bone in which the metastasis of many malignancies is seen (1,2). Sternal metastases are more common than primary malignancies of the sternum. The diseases that most commonly metastasize are breast, lung, kidney, prostate and thyroid cancers (3,4). Computed tomography (CT) is preferred for the evaluation of the sternum anatomy and sternal lesions due to its features of high spatial and contrast resolution and multiplanar reconstruction (5-8). The aim of this study was to evaluate sternal metastases according to the CT characteristics of the thorax and to correlate them with the primary malignancies of patients.

2. Material and Method

Patients that presented to in the last five years were retrospectively screened, and those with sternal lesions on contrast-enhanced CT were

identified. Of the cases with primary malignancies, those showing an involvement in Positron Emission Tomography (PET-CT) or those with widespread bone metastases having newly developed lesions in the sternum or old lesions that progressed to the sternum were accepted as metastases. The measurements and morphological evaluation were performed using the previous CT examination from the time when the first diagnosis of sternal metastases had been made. The density measurement of sternal metastases was performed in the axial sections of the bone window on the CT of the thorax in Hounsfield Unit (HU). The location of metastases was grouped according to sternal anatomy. The size of the lesions was measured from the widest part of the sternal metastases in axial sections. The metastases in the sternum and other non-sternum bones if any were classified as lytic, sclerotic, and mixed. The sternal metastases were grouped according to

their primary malignancy. For sternal metastases, the maximum standard uptake value (SUV_{max}) was measured in PET-CT. When sternum metastases were detected, the presence of metastases in the lung parenchyma was also evaluated. Patients with multiple malignancies were excluded from the study.

Statistical analysis

The data obtained from the study were transferred to a computer and evaluated using the Statistical Package for the Social Sciences (SPSS version 15.0) at the statistical significance value of $p \leq 0.05$. Number, percentage, median, minimum and maximum values were used to evaluate the descriptive data. Lesion density, lesion diameter, and SUV_{max} values were evaluated in terms of compliance with normal distribution, and the Kolmogorov-Smirnov test and graphs revealed that these parameters did not show normal distribution. The Kruskal-Wallis test was used for data analysis.

Our study was approved by the Non-Invasive Clinical Research Ethics Committee of Eskisehir

Osmangazi University of (Date: 10.09.2019 Number: 05).

3. Results

Of the 69 patients, 65.2% (45) were male and 34.8% (24) were female. The primary diagnosis was lung cancer in 29.0% ($n = 20$), prostate cancer in 27.5% ($n=19$) (Fig. 1), and breast cancer in 21.7% ($n = 15$) (Fig. 2). In the sternum localization, the CT imaging revealed the involvement of the corpus in 89.8% ($n = 62$), manubrium in 57.9% ($n = 40$), and xiphoid process in 11.6% ($n = 8$). The maximum lesion density ranged from 26 to 974, with a median of 352. The maximum lesion diameter ranged from 3.0 to 32.1 mm in the axial section, with a median of 11.61 mm. The most common type of metastasis was sclerotic in sternal metastases (60.9%) and multiple sclerotic in non-sternum bones (50.7%). Lytic sternal lesions are less common (Fig. 3). Of the patients, 15.9% ($n = 11$) had metastases both in the sternum and lung parenchyma. The measured SUV_{max} values ranged from 1.4 to 11.0 with a median of 4.0.

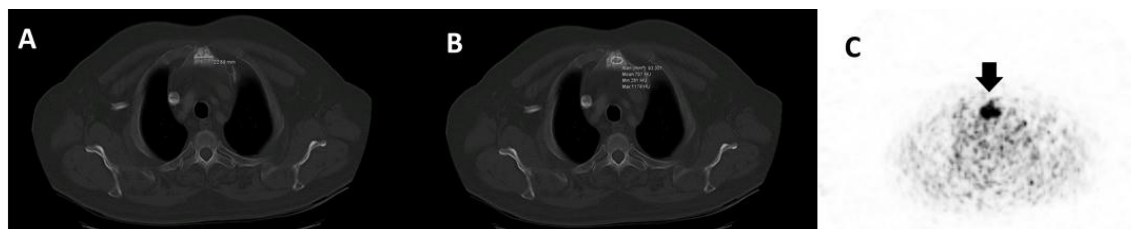


Figure 1. CT images of a prostate cancer case with multiple sclerotic lesions in the body and manubrium of the sternum. Figure 1A shows the measurement of the widest diameter of the lesion in the axial section, Figure 1B demonstrates the measurement of lesion density, and Figure 1C reveals the measurement of SUV_{max} as 4 on PET-CT.



Figure 2. CT images of a breast cancer case with a lytic lesion in the body of the sternum. Figure 2A reveals a lytic lesion with high fluorodeoxyglucose (FDG) uptake measurement of SUV_{max} as 7 on PET-CT, Figure 2B shows the widest part of the lesion in the axial section and and Figure 2C shows the measurement of lesion density.

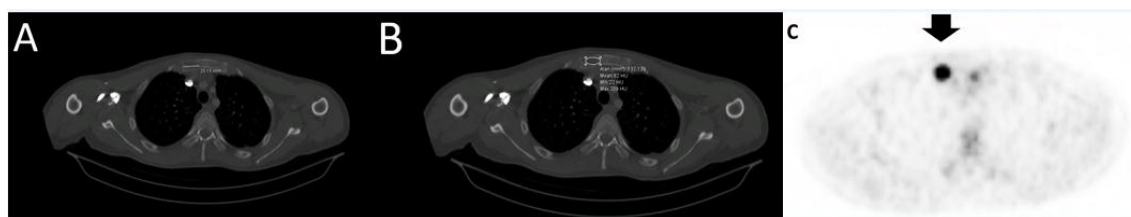


Figure 3. CT images of a well-differentiated liposarcoma case with multiple lytic component-rich lytic-sclerotic metastatic lesions of the manubrium and body of the sternum. The measurements were performed on the widest part of the lesion in the axial section (Figure 3A) and lesion density (Figure 3B) in the bone window. In PET-CT (Figure 3C), the SUV_{max} of the lesion was measured as 10.

Corpus sternum involvement was mostly found in lung cancer, and manubrium and xiphoid involvement in prostate cancer. Sclerotic metastasis involvement was most frequently

seen in prostate cancer. The distribution of cancer cases according to the investigated variables is given in Table 1.

Table 1. Distribution of cancer cases according to the investigated variables

Variable	Primary Diagnosis				
	Lung Cancer n (%)	Prostate Cancer n (%)	Breast Cancer n (%)	Other Cancers n (%)	
Sternal localization on CT					
Corpus	Present	19 (95.0)	18 (94.7)	13 (86.7)	12 (80.0)
	Absent	1 (5.0)	1 (5.3)	2 (13.3)	3 (20.0)
Manubrium	Present	9 (45.0)	14 (73.7)	9 (60.0)	8 (53.3)
	Absent	11 (55.)	5 (26.3)	6 (40.0)	7 (46.7)
Xiphoid	Present	1 (5.0)	4 (21.1)	1 (6.7)	2 (13.3)
	Absent	19 (95.0)	15 (78.9)	14 (93.3)	13 (86.7)
Type of metastasis in the sternum					
Lytic	3 (15.0)	0 (0.0)	2 (13.3)	3 (20.0)	
Sclerotic	13 (65.0)	16 (84.2)	5 (33.4)	8 (53.3)	
Lytic sclerotic	4 (20.0)	3 (15.8)	8 (53.3)	4 (26.7)	
Type of metastasis in non-sternum bones					
Multiple sclerotic	10 (50.0)	18 (94.7)	3 (20.0)	4 (26.7)	
Other	9 (45.0)	1 (5.3)	9 (60.0)	8 (53.3)	
None	1 (5.0)	0 (0.0)	3 (20.0)	3 (20.0)	
Metastasis in the lung parenchyma					
Present	6 (30.0)	1 (5.3)	3 (20.0)	1 (6.7)	
Absent	14 (70.0)	18 (94.7)	12 (80.0)	14 (93.3)	
Total	20 (29.0)	19 (27.6)	15 (21.7)	15 (21.7)	

Lesion density was higher in prostate cancer than other types of cancer. No difference was found between the types of cancer in lesion diameter measured from the axial section. There was also no difference between cancer

types in terms of the measured SUV_{max} values. Table 2 presents the distribution of the patients diagnosed with cancer according to lesion density, lesion diameter, and SUV_{max} values.

Table 2. Distribution of patients with a cancer diagnosis according to lesion density, lesion diameter, and SUV_{max} values

Variable	Primary Diagnosis				Kw/z; p
	Lung Cancer Median (min-max)	Prostate Cancer Median (min-max)	Breast Cancer Median (min-max)	Other Cancers Median (min-max)	
Lesion density	351.5 (58.0-797.0)	472.0 (161.0-974.0)	290.0 (26.0-823.0)	253.0 (31.0-837.0)	9.11; 0.028
Lesion diameter in the axial section	10.7 (4.2-32.1)	10.8 (3.0-28.2)	16.3 (3.4-25.5)	12.1 (3.5-21.1)	1.40; 0.704
SUV _{max} *	4.0 (1.4-7.0)	4.0 (3.0-10.0)	6.0 (3.0-11.0)	4.0 (2.5-10.0)	6.29; 0.098

*Evaluated in a total of 43 patients.

4. Discussion

From the five-year hospital records, the thoracic CT scans of patients with primary malignancies were reviewed and cases with a newly developed lesion in the sternum, those showing an involvement in PET-CT, and those with old lesions progressing to the sternum were accepted as metastases. The primary diagnosis was lung cancer in 29.0% of patients (n = 20), prostate cancer in 27.5% (n = 19), and breast cancer in 21.7% (n = 15). The remaining primary pathologies presenting with sternal metastases evaluated in the 'other' category were liposarcoma, renal cell carcinoma, gastric cancer, neuroendocrine cancer (non-pulmonary origin), rectal cancer, ovarian cancer, thyroid cancer, and mesothelioma.

Using the contrast-enhanced CT of the thorax, lesion density and diameter were measured from the largest lesion in the axial plane and bone window. The maximum lesion diameter ranged from 3.0 to 32.1 mm in the axial section with a median of 11.61 mm. Lee et al. (9) evaluated the sternum metastases of breast cancer using magnetic resonance imaging (MRI) and found the maximum lesion diameter be 1 cm or more in metastases, which is in agreement with our study. In the current study, no significant difference was found between cancer types in terms of lesion diameter measured from the axial section. Schafer et al. and Lee et al. reported that sternal metastases were more likely to be multiple or diffuse in breast cancer cases, and solitary metastases were rarer (9,10).

In the literature, the metastasis of breast cancer to the sternum was detected at a higher rate compared to prostate cancer, while in our study, sternal metastases were higher in

number in prostate cancers (11). In this study, lesion density was higher in prostate cancer than other types of cancer. Sclerotic metastasis was most frequently seen in prostate cancer. Similarly, in the literature, sclerotic metastasis was also most commonly observed in prostate cancer (12,13,14). In prostate cancer, metastasis usually occurs in vertebral and pelvic bones, while vertebra, rib and sternum involvement are most common in breast cancer, and rib and vertebra involvement in lung cancer (11).

The corpus exhibits higher involvement than the xiphoid process and manubrium (2,15). In our study, corpus involvement was the most common localization, which is in agreement with the literature. Therefore, the corpus should be examined more carefully in the metastasis scans of the sternum. Among primary malignancies, sternal metastasis of the corpus was mostly found in lung cancer while manubrium and xiphoid metastases were mostly present in prostate cancer.

There was no difference between cancer types in terms of the measured SUV_{max} values. The SUV_{max} value was 2.5 and above in sternal lesions in all malignancies other than primary lung cancer and ranged from 1.4 to 7 in lung cancer cases.

Of the patients, 15.9% (n = 11) had metastases both in the sternum and lung parenchyma. Among these pathologies, parenchymal metastasis most commonly accompanied lung cancer.

Bone metastases detected in the follow-up of many malignancies are often responsible for

morbidity (16,17), and are therefore crucial to identify. The sternum requires careful attention in screening since the pathologies in this region can easily be overlooked.

The limitations of our study were the small number of patients and the lack of histopathological analysis of sternal lesions.

5. Conclusion

In this study, no significant difference was found between different types of cancer in terms of lesion diameter measured from the axial section on CT. The density measurements revealed that lesion density was higher in

prostate cancer than other types of cancer. There was no difference between cancer types in relation to the measured SUV_{max} values. CT is an important diagnostic tool in the detection of sternal metastases and should be correlated with PET-CT. It should be kept in mind that low SUV_{max} values can be obtained, especially in lung cancer. Among primary malignancies, corpus sternum metastasis was most common in lung cancer and manubrium and xiphoid metastases in prostate cancer. In our study, sternum corpus involvement was the most common localization, and therefore we suggest that the corpus should be carefully evaluated in the scans of sternal metastases.

REFERENCES

1. Altalib AA, Menezes RG. Anatomy, Thorax, Sternum. StatPearls [Internet]. Treasure Island (FL): StatPearls Publishing; 2019-2019 Apr 10.
2. Urovitz EP, Fornasier VL, Czitrom AA. Sternal metastases and associated pathologic fractures. *Thorax* 1977;32:444-8.
3. Restrepo CS, Martinez S, Lemos DF et al. Imaging appearances of the sternum and sternoclavicular joints. *Radiographics* 2009; 29:839-59.
4. O'Sullivan P, O'Dwyer H, Flint J et al. Malignant chest wall neoplasms of bone and cartilage: a pictorial review of CT and MR findings. *Br J Radiol* 2007; 80: 678-84
5. Anuradha Singh, Sheragaru Hanumanthappa Chandrashekhara, Gowramma Sannanaik Triveni, Pawan Kumar. Imaging in Sternal Tumours: A Pictorial Review. *Pol J Radiol* 2017;82:448-56.
6. Goodman LR, Teplick SK, Kay H. Computed tomography of the normal sternum. *AJR Am J Roentgenol* 1983; 141:219-23.
7. Stark P, Jaramillo D. CT of the sternum. *AJR Am J Roentgenol* 1986; 147:72-7.
8. Shin MS, Berland LL, Ho KJ. Computed tomography evaluation of primary and secondary sternal neoplasms. *J Comput Tomogr* 1986; 10:27-32.
9. Lee AY et al. Characterization of Metastatic Sternal Lesions on Dynamic Contrast Enhanced Breast MRI in Women with Invasive Breast Cancer *Acad Radiol* 2019;26:1358-62
10. Schaefer AR, Yang L, Park JM, Xiong J, Fajardo LL. Detection and clinical significance of sternal lesions on breast MRI. *Breast J*. 2015;21:395-402.
11. Vahid Reza Dabbagh Kakhki, Kazem Anvari, Ramin Sadeghi, Anoshe-Sadat Mahmoudian, Maryam Torabian-Kakhki. Pattern and distribution of bone metastases in common malignant tumors. *Nuclear Medicine Review* 2013; 16,2: 66-9.
12. Guise TA, Mohammad KS, Clines G, et al. Basic mechanisms responsible for osteolytic and osteoblastic bone metastases. *Clin Cancer Res* 2006;12:6213-6.
13. Lee RJ, Saylor PJ, Smith MR. Treatment and prevention of bone complications from prostate cancer. *Bone* 2011;48:88-95.
14. Logothetis CJ, Lin SH. Osteoblasts in prostate cancer metastasis to bone. *Nat Rev Cancer* 2005;5:21-8.
15. Otsuka N, Fukunaga M, Morita K, Ono S, Nagai K. Photon-deficient finding in sternum on bone scintigraphy in patients with malignant disease. *Radiat Med* 1990; 8:168-72.
16. Memon AG, Jaleel A, Aftab J. Patten of prostatic carcinoma metastases in bones detected by bone scans using Technitium 99m methyl dipohosphate (Tc99m MDP) imaging technique. *Pak J Med Sci* 2006;22: 180-3.
17. Morgan JWM, Adcock KM, Donohue RE. Distribution of skeletal metastases in prostatic and lung cancer. *Urology* 1990; 36.